

Free Energy Distribution and Relaxation Dynamics Near the First-Order Transition Line

Ranran Guo,¹ Xiaobing Li,^{1,2} Mingmei Xu,^{1,*} Jinghua Fu,¹ and Yuanfang Wu^{1,†}

¹*Key Laboratory of Quark and Lepton Physics (MOE) and Institute of Particle Physics,
Central China Normal University, Wuhan 430079, China*

²*School of Physics and Electronic Engineering, Hubei University of Arts and Sciences, Xiangyang 441053, China*

Using the three-dimensional kinetic Ising model with Metropolis algorithm, we calculate the free energy in the whole phase boundary, particularly near the first phase transition line (1st-PTL). The results show that along the 1st-PTL, as the temperature decreases, the energy barrier between the two coexisting phases diverges. This results in more difficulty to reach the equilibrium, i.e., ultra-slow relaxation, which has been recently demonstrated. Meanwhile, we exam the randomness of the equilibrium time. It is found that near the 1st-PTL the equilibrium time is self-diverging, in contrast to the non-self-averaging near the critical point.

I. INTRODUCTION

Free energy is a fundamental thermodynamic state function that describes the energy available to perform work under specified conditions. It plays a crucial role in the relaxation dynamics of the system and contributes to understanding the stability, phase transition behavior, and critical phenomena of the system in equilibrium [1–5]. The principle of free energy is also widely applied in various fields, including intelligence [6, 7], neuroscience [8, 9], and biological systems [10], making it an essential tool for interdisciplinary research.

The calculation of free energy is primarily determined by a suitable model or Hamiltonian, a sampling protocol, and an estimator of free energy [11, 12]. To accurately capture the behavior of the system, the model or Hamiltonian must reflect the interactions between particles, external fields, and temperature dependencies. The choice of sampling protocol is crucial to generate a representative set of system configurations, ensuring that all relevant microstates are taken into account in the calculation. A variety of methodologies have been employed to compute the free energy in different Ising models, such as mean field approximation (MFA), Monte Carlo (MC) simulations, and methods based on collective variables, each offering different levels of accuracy and computational efficiency.

The MFA primarily provides the distribution of the free energy per spin near the critical point and in small external fields [13]. In the absence of an external field and below the phase transition temperature, the per spin free energy exhibits a double-well structure. Under a small positive external field, both minima shift to the right, with the right one deepening, and the left one becoming shallower. The deeper minimum corresponds to the stable state, while the shallower one represents the metastable state.

Within the MC method for finite-size samples [14], at a temperature close to zero, the restricted free energy is determined by states with minimal energy, and the barrier between its two minima with opposite polarization corresponds to states with two large domains, the inter-face energy of which is proportional to the sample size L .

By extending the results of the collective variables method [15] to the 3D Ising-like model with an external field [3], the Gibbs free energy and Helmholtz free energy can be calculated and establish the regions of stability, metastability, and unstability for the system under investigation.

While the general properties of the free energy are well understood, a comprehensive and detailed study of the free energy characteristics across the entire phase boundary still remains. In this paper, using finite-size samples generated by the Metropolis algorithm, we demonstrate the characteristics of the free energy in the 3D Ising model under a uniform external field at different temperatures.

We provide a presentation of the functional distributions of free energy and magnetization, as well as the changes in the energy barriers between the minima, at different evolution time of the 3D Ising model. The existence of coexistence states and metastable states leads to an increase in the randomness and instability of the system. In our previous work on nonequilibrium evolution [16], the ultra-slow relaxation along the first-order phase transition line (1st-PTL) also reflects this characteristic. Therefore, we further investigated the distribution of free energy at different evolution times to reflect the relaxation characteristics of the system. To evaluate the influence of τ_{eq} on the randomness of the system, we provide the self-averaging principle of τ_{eq} along the first-order phase transition line and reveal the impact of the free energy on the self-averaging properties of the τ_{eq} .

This paper is structured as follows: Section II introduces the kinetic Ising model and calculate method for free energy. Sections III and IV present the simulation results. Section V provides a summary and discussion.

*Electronic address: xumm@cnu.edu.cn

†Electronic address: wuyf@cnu.edu.cn

II. MODEL AND METHOD

The three-dimensional Ising model considers a simple cubic lattice composed of $N = L^3$ spins, where L is called the system size. The state of the system can be represented by a series of spins, i.e., $k = \{s_i\}$, $s_i = \pm 1$, $i = 1, 2, \dots, N$. The total energy of the system in a uniform external field H is

$$E_k = E_{\{s_i\}} = -J \sum_{\langle ij \rangle} s_i s_j - H \sum_{i=1}^N s_i, \quad (1)$$

where J is known as the nearest-neighbor interaction constant between two spins s_i and s_j . For a series of Monte Carlo simulations of the model, E_k represents the total energy of the k^{th} configuration. The energy per spin is

$$\varepsilon_k = \frac{E_k}{N}. \quad (2)$$

The partition function is

$$Z(T, H) = \sum_k \exp(-E_k/k_B T), \quad (3)$$

where k_B is Boltzmann's constant. The free energy is evaluated by

$$F = -k_B T \ln Z. \quad (4)$$

In the 3D Ising model, the large values of E_k cause the exponential function of Z to diverge as E_k increases. Therefore, we choose to use the per-spin average energy ε_k instead of the total energy E_k to calculate the partition function, that is

$$Z(T, H) = \sum_k \exp(-\varepsilon_k/k_B T). \quad (5)$$

And the free energy is

$$F = -k_B T \ln \sum_k \exp(-\varepsilon_k/k_B T). \quad (6)$$

The average total magnetization is

$$M = - \left(\frac{\partial F}{\partial H} \right)_T = \left\langle \sum_{i=1}^N s_i \right\rangle, \quad (7)$$

and the per-spin magnetization is

$$m = \frac{1}{N} \sum_{i=1}^N s_i. \quad (8)$$

It serves as the order parameter of the continuous phase transition at the critical temperature T_c . The most recent shows a high-precision estimate of the critical coupling for the 3D Ising model as $K_c = J/k_B T_c = 0.221654631(8)$ [17, 18]. Usually, J and k_B are set to 1 and the phase boundary is depicted by the line $H = 0$.

Metropolis algorithm, introduced by Nicolas Metropolis [19], is widely used to simulate the process of a system evolving from non-equilibrium to equilibrium. Starting from an initial configuration, the Metropolis algorithm flips one single spin at each step. Whether the chosen spin flips depends on the acceptance probability $A(\mathbf{u} \rightarrow \mathbf{v})$, which is given by

$$A(\mathbf{u} \rightarrow \mathbf{v}) = \begin{cases} e^{-(E_v - E_u)/k_B T} & \text{if } E_v - E_u > 0, \\ 1 & \text{otherwise.} \end{cases} \quad (9)$$

u and v represent the state of the system before and after flipping this spin. If $A(\mathbf{u} \rightarrow \mathbf{v}) = 1$, the spin is flipped. If $A(\mathbf{u} \rightarrow \mathbf{v}) < 1$, a random number r ($0 < r < 1$) is generated. If $A(\mathbf{u} \rightarrow \mathbf{v}) > r$, the spin is flipped, otherwise, the spin keeps its original state.

A Monte Carlo step refers to a single spin-flip attempt, while a sweep represents the completion of one full update cycle involving all N spins in the lattice. The system configuration is updated after each sweep. In subsequent calculations, time t is defined as the number of sweeps.

The stable value of magnetization in an evolution process is a sign of the equilibrium state. Equilibration time of an evolution process is defined by the number of sweeps required for the magnetization m to reach the equilibrium value. Based on our previous work [16], the magnetization fluctuates around the mean value after reaching equilibrium. In practical operation, the mean value and the standard error of the magnetization are calculated and denoted by μ and σ , respectively. The equilibration time τ_{eq} is defined as the moment when the magnetization enters the interval $(\mu - \sigma, \mu + \sigma)$ during the evolution process.

In this study, we utilized the Metropolis algorithm to simulate the evolution of the 3D Ising model with periodic boundary conditions, transitioning from non-equilibrium to equilibrium under a uniform external field.

To analyze the variations in free energy F and magnetization per spin m , we generate ten thousand samples for each temperature and evolution time. The data processing procedure is as follows:

(1) Divide the ten thousand magnetization samples m_k for each temperature T into 10 equal-width bins arranged in ascending order, while simultaneously assigning the per-spin average energy ε_k of each sample to the bin corresponding to its magnetization m_k .

(2) Calculate the partition function Z in each bin according to Eq. 5.

(3) Calculate the free energy F in each bin according to Eq. 6 and get the curve of F with m is obtained.

III. THE CHARACTERISTICS OF THE FREE ENERGY NEAR THE ENTIRE PHASE BOUNDARY

When $H = 0$, the system evolves from a random configuration to different temperatures. The complete variation of the free energy F as a function of average order

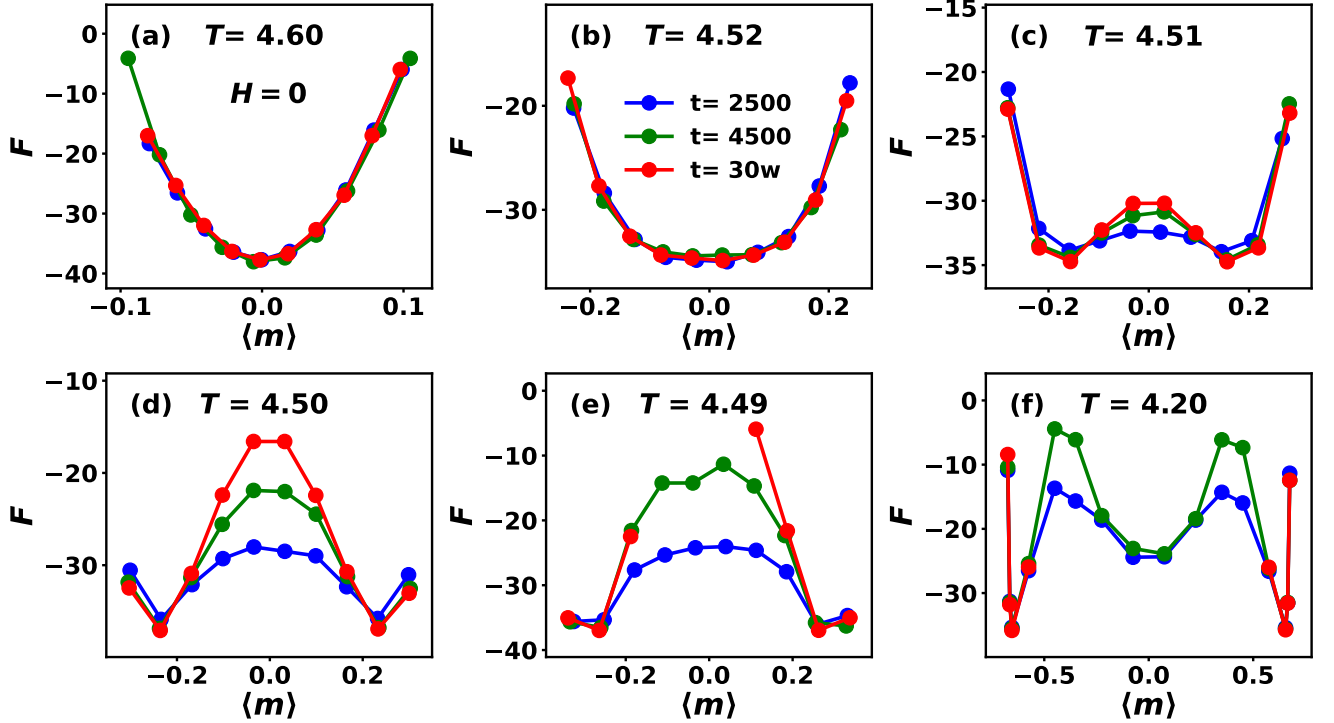


FIG. 1: (color online) The free energy F as a function of the average order parameter $\langle m \rangle$ for six different temperatures at $H = 0$. The selection of six different temperatures span the entire phase transition line. The lattice size L is 60.

parameter $\langle m \rangle$ along the phase transition line is shown at three evolution times in Fig. 1. The three evolution times include $t = 2500$ (blue circles), where most low-temperature systems have not yet reached equilibrium; $t = 4500$ (green circles), at which equilibrium is observed in some systems; and $t = 300000$ (red circles), by which time all systems have reached dynamic equilibrium.

In Fig. 1(a), for a system with temperature $T \gg T_c$, i.e., $T = 4.60$, F as a function of $\langle m \rangle$ exhibits a V-shaped variation at evolution time $t = 2500$. A local minimum appears at $m = 0$ within the magnetization range. As the evolution time t increases to 4500 or 300000, the overall trend of F as a function of $\langle m \rangle$ remains unchanged. According to the second law of thermodynamics, a system evolves toward the minimization of its free energy. When F reaches its minimum value, the system is in thermodynamic equilibrium, denoted as F_{min} . Therefore, as shown in Fig. 1(a), at high temperatures, the stable equilibrium state of the system corresponds to the disordered phase ($m = 0$).

In Fig. 1(b), the system temperature is $T = 4.52$. At an evolution time of $t = 2500$, the free energy F exhibits a U shaped symmetrical pattern with respect to $\langle m \rangle$, characterized by a wide and flattened minimum. The extended flatness of the potential base indicates that near criticality, the free energy remains nearly degenerate across a wide magnetization range, reflecting critical softening of the energy barrier. When the evolution time extends to $t = 4500$ or $t = 300000$, the $F(m)$ profile retains its char-

acteristic symmetry and flat-bottomed topology, demonstrating the persistence of critical scaling behavior under prolonged temporal evolution.

In Figs. 1(c) - (d), at temperatures $T = 4.51$ and $T = 4.50$, the free energy F exhibits two equivalent minima within the magnetization range, forming a symmetric double-well structure. As the evolution time increases to $t = 4500$ or $t = 300000$, the overall trend of F as a function of $\langle m \rangle$ remains unchanged. Despite significant fluctuation in $\langle m \rangle$, the free energy F reveals two minima within the magnetization range over a sufficiently long evolution time. The two minima correspond to the coexistence of two phases, consistent with the predictions of the Landau-Ginzburg mean-field theory for $T < T_c$. Between these two minima, F reaches a maximum near $m = 0$, which represents the energy barrier separating the two phases. The energy barrier between the two phases increases as the temperature decreases.

As shown in Fig. 1 (e), the temperature decreases further to $T = 4.49$. At evolution times $t = 2500$ and $t = 4500$, F exhibits two equivalent local minima and a maximum within the distribution range of $\langle m \rangle$. When the evolution time reaches $t = 300000$, F still has two equivalent local minima, but the maximum disappears and F no longer has values over a wide range of $\langle m \rangle$. This indicates a sharp increase in the energy barrier between the two phases.

When the temperature decreases to $T = 4.20$, F exhibits an M-shaped symmetric trend with respect to $\langle m \rangle$

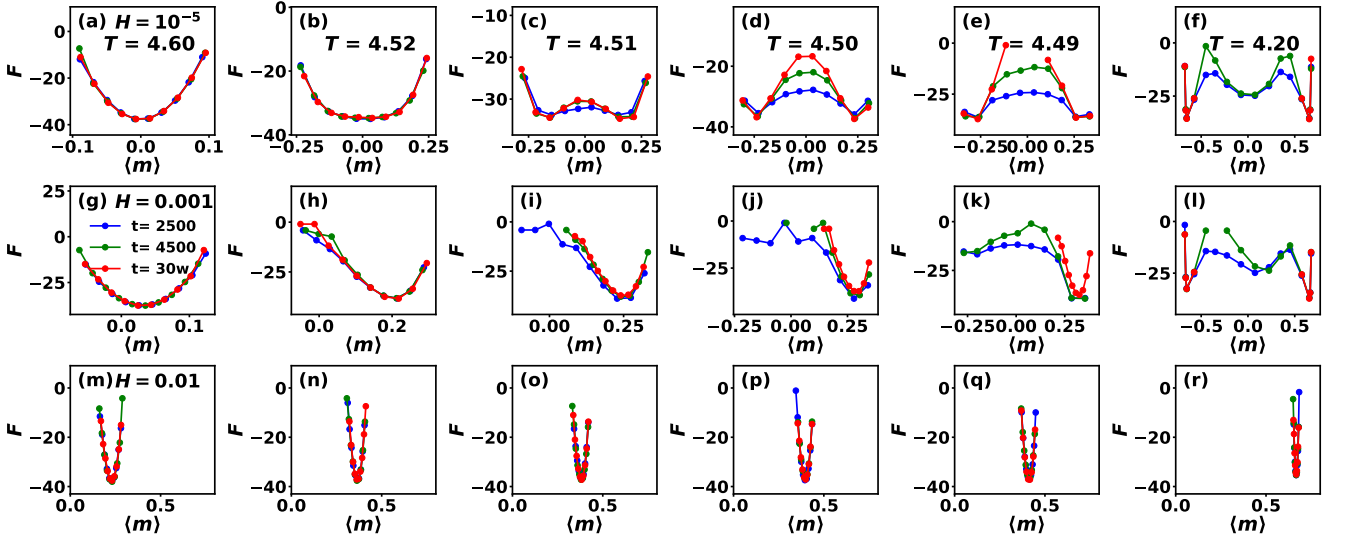


FIG. 2: The free energy F as a function of the average order parameter $\langle m \rangle$ for six temperatures at three different external fields. The first row corresponds to $H = 10^{-5}$, the second row corresponds to $H = 0.001$, and the third row corresponds to $H = 0.01$. The lattice size L is 60.

at $t = 2500$, with two minima corresponding to the maximum magnetization m_{max} and the minimum magnetization m_{min} . At $t = 4500$, the trend of F with respect to $\langle m \rangle$ remains unchanged. When the evolution time becomes sufficiently large, i.e., $t = 300000$, the free energy F takes values only at m_{max} and m_{min} . To better capture the characteristics of the local data, the data was further binned, revealing the changes in the distribution of the free energy F in the inset of Fig. 1(f). The distribution of F with respect to $\langle m \rangle$ is symmetric about $m = 0$, with two minima appearing on either side of the $\langle m \rangle$ -interval. These two minima correspond to stable two-phase coexistence states. Between these two-phase coexistence states, F does not take any value, indicating that the barrier between the two phases tends to infinity.

In a word, as the temperature decreases along the phase boundary, a transition from a single minimum to two minima in free energy occurs at the 1st-PTL. As the temperature drops near the CP, the distribution of F changes from narrow V-shaped to broader U-shaped. This change typically reflects the transition of the equilibrium state from an disordered phase to the critical region as the temperature decreases, with an increase in system uncertainty and a diminishing difference between different magnetization values. Additionally, the free energy distributions exhibit consistent trends across various evolution times, except at $T = 4.20$. When T decreases along the 1st-PTL, the barrier between the two free energy minima gradually increases to infinity. The trends of the free energy distribution exhibit significant variation with different evolution times, as the time required for the system to reach full equilibrium increases. These findings are consistent with our earlier study [16], indicating that the existence of coexistence states along the 1st-PTL significantly increases the instability, leading to

a longer equilibration time.

In order to see the distribution characteristics of the free energy near the phase boundary, Fig. 2 presents the free energy distributions at different evolution times under three external fields.

For the small field, i.e., $H = 10^{-5}$, the variation of F with $\langle m \rangle$ at each temperature remains consistent with that observed at $H = 0$, as shown in the first row of Fig. 2. When H increases to 0.001 or 0.01, leaving the phase boundary further, the distribution of F with respect to $\langle m \rangle$ exhibits significant changes at different temperatures. Apart from the two minima becoming unequal, the larger minimum corresponds to the metastable state and the smaller minimum represents the stable state.

The second row of Fig. 2 shows the free energy distribution under an external field $H = 0.001$.

When the temperature is above the critical temperature, as shown in Fig. 2(g) and Fig. 2(h), the free energy F distribution exhibits a skewed V-shape, with the minimum corresponding to a positive value of $\langle m \rangle$. The free energy distributions at three different times overlap, indicating that the system reaches equilibrium quickly.

As the temperature falls below the critical temperature, as shown in Fig. 2(i) to Fig. 2(k), the trend of F with $\langle m \rangle$ no longer exhibits a double-well shape. At evolution times of 2500 and 4500, the trend of F with $\langle m \rangle$ in Fig. 2(k) deviates from the symmetric double-well shape, showing two unequal minima. The free energy F exhibits a skewed V-shaped distribution, with the minimum corresponding to a positive value of $\langle m \rangle$, indicating that the system reaches a stable equilibrium state in the ordered phase at $t = 300000$.

At low temperature $T = 4.20$, the distribution of F is no longer symmetric about $m = 0$ and F exhibits two

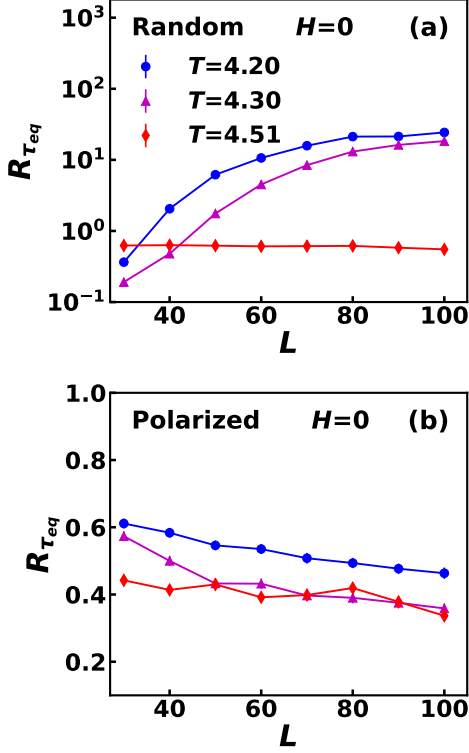


FIG. 3: $R_{\tau_{eq}}$ as a function of L for different initial states: random initial state(a), polarized initial state(b.)

unequal minima in Fig. 2(l). The right minimum is lower than the left, indicating that the former corresponds to a stable equilibrium state, while the latter represents a metastable state.

The third row of Fig. 2 presents the distribution of F with $\langle m \rangle$ at $H = 0.01$. Throughout the temperature range, the free energy F exhibits a sharp V-shaped distribution, with the minimum corresponding to a positive value of $\langle m \rangle$. The distribution of free energy overlaps at different evolution times, indicating that the system reaches equilibrium quickly.

Near the phase boundary, when the external field is small, the trend of F at each temperature remains similar to that observed at $H = 0$, except that the two minima become unequal along the 1st-PTL. The smaller minimum corresponds to the stable state, while the larger one represents the metastable state. When the external field is sufficiently large, the system stabilizes into a single ordered phase aligned with the field direction, where no phase transition characteristics, coexistence states, or metastable states are observed. Furthermore, the distribution of F at different evolution times overlaps, indicating that the system reaches complete equilibrium in a short time.

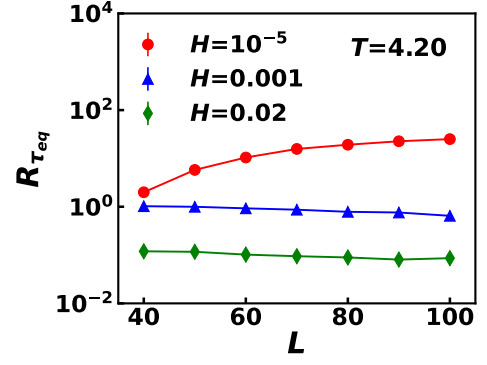


FIG. 4: The relative variance of $R_{\tau_{eq}}$ as a function of system size for three different values of the external magnetic field at $T = 4.20$

IV. THE SELF-AVERAGING PROPERTIES OF EQUILIBRATION TIME

The free energy structure exhibits significant differences near the critical point and along the first-order phase transition line, corresponding to changes in the system's relaxation time. To evaluate the influence of evolution time on the randomness of the system, the equilibrium time τ_{eq} is measured at various temperatures and system sizes. To demonstrate the random variation of τ_{eq} along the entire phase boundary, we examine the self-averaging property of τ_{eq} .

Self-averaging refers to the behavior of the relative variance of an observable X as the system size increases. It is defined as follows [20]:

$$R_X = \frac{\overline{X^2} - \overline{X}^2}{\overline{X}^2}, \quad (10)$$

where bar represents the average over the entire samples. If R_X tends to zero, X is self-averaging; if R_X increases, X is self-diverging. In case of self-averaging, the fluctuation of X diminishes as the system size increases, and the average of X converges to the same value. Self-diverging means divergent fluctuations of X as the system size increases.

At the phase boundary, the relative variance of τ_{eq} starting from a random initial state is plotted against the system size for three different temperatures in Fig. 3(a). The trend of $R_{\tau_{eq}}$ is obviously different for each of temperature cases.

At temperature $T = 4.51$, $R_{\tau_{eq}}$ remains almost constant as the system size increases. In other words, the variance or width of τ_{eq} distribution increases with the system size at the same rate as the average of τ_{eq} , indicating non-self-averaging behavior of τ_{eq} , consistent with other observables [20].

At two lower temperatures $T = 4.30$ and $T = 4.20$, $R_{\tau_{eq}}$ increases with system size, indicating self-diverging behavior at the 1st-PTL, similar to what is observed in liquid crystals [21]. As the system size increases, the

variance of τ_{eq} increases more rapidly than the average of τ_{eq} , and the distribution of τ_{eq} becomes wider and flatter. This phenomenon suggests that randomness is significantly amplified with system size, leading to an abnormally increased variance. Such an extremely broad distribution of τ_{eq} is the ultra-slow relaxation along the 1st-PTL.

Figure 3(b) presents the relative variance of τ_{eq} starting from a polarized initial state. It demonstrates that the relative variance of τ_{eq} decreases with system size for all three temperatures, indicating that τ_{eq} exhibits self-averaging behavior in this case.

As we know, if starting from upward polarized initial configurations with $m(0) = 1$, $\langle m \rangle$ is bound to decrease quickly to the right minimum. The polarized initial configuration is equivalent to an equilibrium state at a very low temperature. Consequently, the evolution from a polarized initial configuration to the states in the large external field is facile, resulting in a substantial reduction in the time required for the system to reach a complete steady state, as observed in Fig. 2 for $H = 0.01$.

To investigate behavior beyond the phase boundary, Fig. 4 illustrates the relative variance of $R_{\tau_{eq}}$ at a constant temperature $T = 4.20$, plotted against different system sizes for three distinct external fields. The external fields are $H = 10^{-5}$ (red circles), $H = 0.001$ (blue triangles), and $H = 0.02$ (green rhombuses).

It is observed that self-diverging behavior is only prominent at $H = 10^{-5}$, which is the nearest to the 1st-PTL in Fig. 4. For larger external fields, such as $H = 0.001$ and $H = 0.02$, $R_{\tau_{eq}}$ decreases slowly as L increases, indicating the self-averaging of τ_{eq} . As the deviation from the 1st-PTL becomes further, the self-diverging behavior of τ_{eq} becomes less pronounced. Therefore, self-diverging behavior is observed not only precisely at the 1st-PTL but also in its close vicinity, while far from the phase boundary, τ_{eq} exhibits self-averaging behavior.

At the phase boundary with random initial state, the self-averaging behavior of τ_{eq} is consistent with the distribution characteristics of the free energy in Fig. 1. The appearance of coexistence states at $T = 4.51$ increases the randomness of the system and leads to an increase in the evolution time required for the system to reach complete equilibrium. The non-self-averaging behavior of τ_{eq} is consistent with the fluctuations arising from the coexisting states. At lower temperature $T = 4.20$, the differences in the distribution of F at different evolution times increase. As the system reaches complete stability, the barriers between coexisting states tend towards infinity. This implies an increase in the randomness and uncertainty of the system, which is consistent with the self-divergent nature of τ_{eq} at this stage. Compared to near the critical point, τ_{eq} at low temperatures exhibits self-diverging, further confirming that extremely slow relaxation dynamics occur along the first-order phase transition line.

V. SUMMARY AND DISCUSSION

In this paper, we investigate the free energy of the three-dimensional kinetic Ising model using the Metropolis algorithm. The characteristics of the free energy are systematically presented for the first time near the entire phase boundary, considering various external fields, temperatures, and evolution times.

As the temperature decreases along the phase boundary, a transition from a single minimum to two minima in free energy occurs at the 1st-PTL. As the temperature drops near the CP, the distribution of F changes from narrow V-shaped to broader U-shaped. Furthermore, the free energy distributions exhibit consistent trends across various evolution times. When T decreases along the 1st-PTL, the barrier between the two free energy minima gradually increases to infinity. The trends of the free energy distribution exhibit significant variation with different evolution times, as the time required for the system to reach full equilibrium increases.

Near the phase boundary ($H = 10^{-5}$), the free energy distribution across temperatures is consistent with that at $H = 0$. With increasing external field, the coexistence and metastable states of free energy gradually disappear, and the system reaches equilibrium more rapidly. For $H = 0.001$, a single minimum in free energy is observed at most temperatures, except at the extremely low temperature of $T = 4.20$, where two unequal minima indicate a stable equilibrium and a metastable state. At $H = 0.01$, the free energy consistently exhibits a single minimum across all temperatures, maintaining positive magnetization and system stability.

The coexistence and metastable states increase the uncertainty and randomness of the system, reflected by a longer τ_{eq} . The relative variance of τ_{eq} is analyzed to examine randomness.

As the system size increases, the relative variance of τ_{eq} increases at the 1st-PTL, and keeps to a constant at the CP. So τ_{eq} exhibits a self-diverging behavior at the 1st-PTL, in contrast to the non-self-averaging at the CP. The increased randomness at the 1st-PTL arises from coexistence states, which expand the number of possible states and consequently lead to a very broad distribution of τ_{eq} . This characteristic of relaxation at the 1st-PTL distinguishes itself from that observed at the CP.

Approaching the phase boundary, the randomness increases due to the appearance of metastable state and τ_{eq} exhibits the self-diverging behavior. Away from the phase boundary, the coexistence and metastable states disappear and the self-averaging behavior of τ_{eq} changes from self-diverging to self-averaging.

The distribution of coexistence and metastable states in free energy reveals the reason why the equilibrium time along the 1st-PTL is longer than at the CP. This result further confirms the significance of equilibrium time in understanding nonequilibrium effects and identifying phase boundaries.

Acknowledgments

We are grateful to Dr. Yanhua Zhang for very helpful discussions. This research was funded by the National Key Research and Development Program of China, grant

number 2022YFA1604900, and the National Natural Science Foundation of China, grant number 12275102. The numerical simulations have been performed on the GPU cluster in the Nuclear Science Computing Center at Central China Normal University (NSC3).

-
- [1] M. Xu and Y. Wu, *Symmetry* **15**, 10.3390/sym15020510 (2023).
 - [2] T. Mori, *Phys. Rev. Res.* **3**, 043137 (2021).
 - [3] M. P. Kozlovskii and R. V. Romanik, *Condens. Matter. Phys.* **14**, 43002 (2011).
 - [4] V. A. Abalmasov, *SciPost Phys.* **16**, 151 (2024).
 - [5] M. KOLESIK, M. A. NOVOTNY, and P. A. RIKVOLD, *International Journal of Modern Physics C* **14**, 121 (2003), <https://doi.org/10.1142/S0129183103004279>.
 - [6] S. T. Jose and O. Simeone, *IEEE Signal Processing Magazine* **38**, 120 (2021).
 - [7] K. Friston, L. Da Costa, N. Sajid, C. Heins, K. Ueltzhöffer, G. A. Pavliotis, and T. Parr, *Physics Reports* **1024**, 1 (2023), the free energy principle made simpler but not too simple.
 - [8] M. J. D. Ramstead, P. B. Badcock, and K. J. Friston, *Physics of Life Reviews* **24**, 1 (2018).
 - [9] N. Hansen and W. F. van Gunsteren, *Journal of Chemical Theory and Computation* **10**, 2632 (2014), pMID: 26586503.
 - [10] M. Colombo and P. Palacios, *Biology & Philosophy* **36**, 41 (2021).
 - [11] M. Mezei and D. Beveridge, *Annals of the New York Academy of Sciences* **482**, 1 (1986).
 - [12] C. D. Christ, A. E. Mark, and W. F. Van Gunsteren, *Journal of computational chemistry* **31**, 1569 (2010).
 - [13] R. B. Griffiths, C.-Y. Weng, and J. S. Langer, *Phys. Rev.* **149**, 301 (1966).
 - [14] K. Binder, *Philosophical Magazine Letters* **87**, 799 (2007), <https://doi.org/10.1080/09500830701496560>.
 - [15] I. R. Y. KII, *La Rivista del Nuovo Cimento* **12**, 1 (1989).
 - [16] X. Li, M. Xu, Y. Zhang, Z. Li, Y. Zhou, J. Fu, and Y. Wu, *Phys. Rev. C* **105**, 064904 (2022).
 - [17] A. M. Ferrenberg, J. Xu, and D. P. Landau, *Phys. Rev. E* **97**, 043301 (2018).
 - [18] P. Hou, S. Fang, J. Wang, H. Hu, and Y. Deng, *Phys. Rev. E* **99**, 042150 (2019).
 - [19] N. Metropolis, A. W. Rosenbluth, M. N. Rosenbluth, A. H. Teller, and E. Teller, *J. Chem. Phys.* **21**, 1087 (1953).
 - [20] S. Wiseman and E. Domany, *Phys. Rev. E* **52**, 3469 (1995).
 - [21] J. M. Fish and R. L. C. Vink, *Phys. Rev. Lett.* **105**, 147801 (2010).